

**THE APPLICATION OF PHYSIOLOGICAL LOADING USING A DYNAMIC, MULTI-AXIS
SPINE SIMULATOR**

Timothy Patrick Holsgrove^{1,2}, Anthony W Miles¹, Sabina Gheduzzi¹

¹Centre for Orthopaedic Biomechanics, Department of Mechanical Engineering, University of
Bath, Bath, BA1 7AY, UK

²College of Engineering, Mathematics & Applied Sciences, University of Exeter, Harrison
Building, Streatham Campus, North Park Road, Exeter, EX4 4QF, UK

Corresponding author:

Timothy Patrick Holsgrove

College of Engineering, Mathematics & Applied Sciences, University of Exeter, Harrison
Building, Streatham Campus, North Park Road, Exeter, EX4 4QF, UK

Telephone: +44 1392 723628

Email: t.holsgrove@exeter.ac.uk

ABSTRACT

In-vitro testing protocols used for spine studies should replicate the in-vivo load environment as closely as possible. Unconstrained moments are regularly employed to test spinal specimens in-vitro, but applying such loads dynamically using an active six-axis testing system remains a challenge. The aim of this study was to assess the capability of a custom-developed spine simulator to apply dynamic unconstrained moments with an axial preload.

Flexion-extension, lateral bending, and axial rotation were applied to an L5/L6 porcine specimen at 0.1 and 0.3 Hz. Non-principal moments and shear forces were minimized using load control. A 500 N axial load was applied prior to tests, and held stationary during testing to assess the effect of rotational motion on axial load.

Non-principal loads were minimized to within the load cell noise-floor at 0.1 Hz, and within two-times the load-cell noise-floor in all but two cases at 0.3 Hz. The adoption of position control in axial compression-extension resulted in axial loads with qualitative similarities to in-vivo data.

This study successfully applied dynamic, unconstrained moments with a physiological preload using a six-axis control system. Future studies will investigate the application of dynamic load vectors, multi-segment specimens, and assess the effect of injury and degeneration.

KEYWORDS

Spine biomechanics; six-axis; dynamic; preload; physiological testing

INTRODUCTION

In-vivo loading of the spine must be accurately replicated in the laboratory setting in order to accurately define the mechanical properties of spinal tissue, and investigate the efficacy of treatments for spinal injury and degeneration [1]. The complexity of the spine, arising from the triple joint structure at each level, and the large number of stabilizing and actuating muscles, means that simulating the in-vivo environment remains a difficult task to achieve [1, 2].

Significant research has been carried out in the development of spine testing systems and, in particular, six-axis testing machines. The stiffening effect of applying a physiological preload on spinal specimens has been well-documented [3-6], with an axial preload leading to an increase in disc stiffness in axial compression-tension, flexion-extension and lateral bending ranging from 100 % to as much as 500 % [6]. The effect of frequency also leads to significant changes in the stiffness of spinal specimens [7, 8]. Costi et al. have reported a linear increase in stiffness against log-frequency increase in testing speed [7]. Previous research has made use of clutches in the non-principal axes in order to impose dynamic pure moments with a physiological preload applied via muscle force simulation [9]. A six-axis test system using position control was also developed to investigate the mechanism of disc herniation [10], demonstrating the importance in complex loading to replicate the in-vivo scenario. Likewise, in recent years there has been an increased focus on the development of testing machines with six-axis load control systems to actively control the load in each axis (Table 1). Such developments offer exciting prospects for the real-time application of complex, biofidelic loading vectors, and provide a means to accomplish the future research objectives outlined by Oxland [11] in more fully understanding disc non-linearity, dynamic effects on the spine, and create more robust links between in-vivo and in-vitro data. However, the testing rate of such machines has thus far been limited, with no system capable of completing tests in flexion-extension, lateral bending, and axial rotation within the

0.5-5.0 °/s testing speed recommended by Wilke et al. [2]. Furthermore, the application of an ideal follower load has been limited to tests in the sagittal plane at 0.35 °/s [12, 13].

It is well-known that spinal posture affects the axial load through the spine, resulting in increased intradiscal pressure [14, 15]. However, when a preload is applied to pure moment testing in-vitro, it is generally maintained at a constant magnitude by means of an axial preload or passive follower-load [4, 16-19], and only recently has an ideal follower-load of physiological magnitude been adopted using an advanced testing system [12, 13]. However, the stiffness matrix testing of spinal specimens has demonstrated that flexion-extension about a fixed position does lead to substantial changes in axial load [6]. It is possible that maintaining the axial position during the application of otherwise unconstrained moments may lead to physiologically representative axial loads being applied to spinal specimens.

The aim of this research was to determine whether a custom-developed spine simulator was able to operate dynamically with an axial preload to complete physiological loading regimes with off-axis moments and shear forces minimized through load control using a porcine lumbar spinal specimen. Success was determined by the ability of the system to complete tests with positional demand errors close to the system resolution, and as previously used as pass criteria in such tests, zero load demand errors within two-times the load cell noise floor [20]. Additionally, the change in axial load due to rotational motion will be discussed in relation to previously published in-vivo data of the intradiscal pressure of the intervertebral disc in different postures [15, 21-23]. Achieving these objectives would demonstrate the test system capabilities to complete complex in-vitro loading regimes, which will improve the ability to replicate in-vivo loads to study the effects of injury, degeneration, and treatment of the spine.

MATERIALS AND METHODS

Test Apparatus

A previously developed dynamic six-axis spine simulator [24] was upgraded to operate as a six-axis electromechanical spine simulator with fully integrated control system (dSPACE Ltd., Melbourn, UK) allowing real-time test capabilities in both load and position control (Figure 1) (Table 2). A vertical axis provided translations in axial compression-tension (TZ), an XY platform provided translations in anterior-posterior shear (TX) and lateral shear (TY), and a gimbal head provided rotations in lateral bending, flexion-extension, and axial rotation (RX, RY, and RZ respectively) (Figure 2). A cranial specimen holder was fixed to the gimbal head, and a caudal specimen holder was fixed to the base plate via a six-axis load cell (AMTI MC3-A-1000, Advanced Mechanical Technology Inc., MA, USA). A previous study had established that the load cell had a noise floor of 5 N and 0.25 Nm [6]. The six-axis assembly was mounted on a crosshead (XH) to allow the vertical adjustment necessary to accommodate specimens of varying lengths.

Test Protocol

Biomechanical tests were completed in flexion-extension, lateral bending, and axial rotation over physiological ROMs at two dynamic frequencies (0.1 and 0.3 Hz). The ROMs used to test each axis (Figure 2) were within the physiological limits measured in-vivo [25, 26], and the same as used previously in the literature [6, 24, 27]: ± 3 mm in TX; ± 1.5 mm in TY; ± 0.4 mm in TZ; and $\pm 4^\circ$ in RX, RY, and RZ. The frequencies were chosen to approximately cover the range recommended [2] of 0.5-5°/sec, whilst also allowing comparisons to previous tests in the literature [6, 24, 28, 29] (Table 1). The frequencies of 0.1 and 0.3 Hz equated to rotational speeds of 1.6 and 4.8°/sec respectively.

The principal axis was operated in position control to ensure a consistent test rate, and negate viscoelastic effects. The non-principal axes were maintained in load control with a

demand of 0 N or 0 Nm, with the exception of the axial compression-tension axis (TZ), which was equilibrated in load control, but was held stationary in position during testing to assess the variance bending on the axial load in relation to previous in-vivo data [14, 15].

Each test comprised five triangular wave cycles, with the first two cycles used for preconditioning [2], and the last three cycles used for data analysis [6, 24]. Position and load data were acquired at 100 Hz for all tests. A 60 second equilibration/recovery period was used prior to each test, with the control mode (position or load) of each axis set to that required for the forthcoming test. This allowed the non-principal loads to be minimized prior to the start of a test, and provided time for system stabilization due to the required control mode changes. The 500 N preload to replicate the load under normal standing posture [14] was equilibrated for 15 minutes prior to testing, and was adjusted throughout the recovery periods but a fixed axial position was maintained during testing. With the aim of providing a greater test of the system capability, no manual adjustments of the TX or TY axes to minimize non-principal moments due to the preload application relative to the specimen center of rotation (COR) were made during the equilibration or recovery periods. The test protocol was completed using an automated script developed in dSPACE ControlDesk, which ensured the timing of all tests and equilibration periods were consistent.

Specimen Preparation

One porcine L5/L6 anterior column unit (ACU) specimen was prepared from a T12-S1 spine; the processes and all musculature were removed, leaving the L5 and L6 vertebral bodies linked via the L5/L6 intervertebral disc, and intact anterior and posterior longitudinal ligaments. A self-tapping screw was driven into the cranial endplate of the L5 vertebra to assist with subsequent identification. The specimen was both sprayed with and wrapped in paper towel soaked with 0.9 % saline solution, triple sealed in plastic bags, and stored at -24 °C until the day of testing.

On the day of testing, the specimen was sprayed with 0.9 % saline whilst still wrapped in the saline soaked paper towel, resealed in three plastic bags, and allowed to thaw for 3 hours at room temperature. During the last hour of thawing the specimen was removed from the plastic bags. To aid fixation when potted using low melting point alloy (MCP75, Mining & Chemical Products Ltd., Northamptonshire, UK), two additional screws were driven into the cranial endplate of the L5 vertebra, and three screws were driven into the caudal endplate of the L6 vertebra. Specimen pots were water cooled during potting to prevent overheating of the specimen, and care was taken to align the intervertebral disc in the horizontal plane. The specimen was mounted in the spine simulator with the centre of the intervertebral disc corresponding to the datum of the displacement axes. The specimen was sprayed with 0.9 % saline solution, wrapped in paper towel soaked with 0.9 % saline solution, and then wrapped in food packaging plastic. Once the specimen was fixed in the simulator, the position of all axes were adjusted to minimize the loads, with the resulting position defined as the neutral position. The testing protocol was then completed at 0.1 and 0.3 Hz with a 500 N axial preload at room temperature.

Data Analysis

Analyses of all data were completed separately for each of the last three test cycles. This approach was adopted to ensure that two preconditioning cycles were sufficient to obtain consistent simulator performance and reliable mechanical data of the spinal specimen.

The tracking error (TE) was calculated using the root mean squared (RMS) error of the actual position relative to the desired position signal. The RMS load error was calculated for non-primary axes with a zero load demand. Non-principal terms with a RMS load error within two times the load cell noise floor were considered to have been successfully maintained at acceptably low levels [20].

Load data were also used to determine the stiffness matrix for the principal axes using the linear least squares (LLS) method [6, 27]. The positive and negative phases were calculated separately for all terms for each of the last three cycles over the entirety of the applied ROM, with the results presented separately for flexion and extension, and the results of the positive and negative phases combined for lateral bending and axial rotation. The stiffness in the TZ axis was also determined for each test, to assess the effect of motion in the principal axes on the axial load.

RESULTS

Control Analysis

The TE of the principal axis operated in position control was maintained within the resolution of the system in all tests, and non-principal axes operated in load control were within two-times the noise floor of the load cell in all but two cases (Table 3). The equilibration/recovery periods and two preconditioning cycles were sufficient to produce consistent behaviour over the last three cycles (Table 3).

At 0.1 Hz, the RMS error of axes with a zero-load demand was maintained within in the noise-floor of the load cell (Figure 3). At 0.3 Hz, the RMS error of the shear forces was maintained within the noise-floor, as were three moments. One moment was within two-times the noise-floor, and the flexion-extension moments due to lateral bending and axial rotation exceeded this limit (Table 3).

Biomechanical Analysis

The stiffness calculated for each of the last three test cycles was consistent, with a typical standard deviation of 0.02-0.03 Nm/°, and a maximum of 0.07 Nm/° in lateral bending at 0.1 Hz (Table 4).

The R^2 values at 0.1 Hz were 0.829 or greater, and reached 0.945 in flexion. Whilst flexion and axial rotation produced similarly linear response at 0.3 Hz (Table 4), the R^2 values in extension and lateral bending were much lower.

Axial compression was altered as a result of rotations (Figure 4), and the effect was greatest in flexion-extension, and lowest in axial rotation (Table 5). The change in axial force demonstrated a good linear relationship in the positive and negative phases of tests, with R^2 values of between 0.820 and 0.928 across tests in all axes at both 0.1 and 0.3 Hz (Table 5), and the stiffness remained consistent over the three tests cycles analyzed. The lateral bending and axial rotation demonstrated greater relaxation than flexion and extension over the last three tests cycles (Figure 4).

DISCUSSION

The aim of the present study was to assess the capability of a six-axis spine simulator to apply dynamic rotational loading with a physiological preload, whilst minimizing off-axis moments and shear force. An additional aim was to assess the effect of rotation on the axial load under a fixed vertical position. The key development from previous work was that tests were completed with non-principal axes being actively controlled, at physiologically dynamic testing rates. A single porcine lumbar spinal specimen was tested; this limits the application of the results in clearly defining the mechanical properties of porcine spinal specimens, or assessing the capability of the spine simulator to robustly adapt to the variability of different specimens, but is comparable with previous tests used to evaluate new spine testing machines using a single specimen [9, 20, 24, 27, 30]. The specimen used comprised a functional spinal unit with the posterior elements removed; this is also a limitation in that it omits the potential coupling effects of the facet joints and posterior ligamentous structures, and the increased complexity of multi-level specimen, which future studies with this test system should address.

The tests demonstrated the ability of the spine simulator to accurately and repeatably operate in position control, and to provide consistent load control under dynamic conditions. This was the case even with the increased difficulty of coupled loading due to the application of an axial preload, without the COR being first estimated to minimize such loads [20]. The application of the preload resulted in a flexion moment of approximately 1 Nm at zero degrees during testing, resulting in a flexion moment even when a rotation of 4° of extension was applied (Figure 3). This flexion moment also led to increased difficulty in minimizing the flexion-extension moment when operating the axis in load control compared to lateral bending and axial rotation. Whilst non-principal moments were maintained within acceptable limits at 0.1 Hz, adjusting the TX and TY axes to ensure the preload is applied through the COR in the neutral position is recommended for future studies. It is likely that this will minimize the artefact moments, whilst also providing more physiologically relevant test data.

The lower R^2 values in extension and lateral bending may have been the result of the lower stiffness measured in these axes compared to flexion, and axial rotation, despite the plots demonstrating reasonably linear relationships over the ROM applied (Figure 3). However, if future tests are conducted over greater ROMs than the present study, the non-linearity of spinal specimens should be accounted for in the method used to calculate specimen stiffness.

The stiffness of the porcine specimen demonstrated comparable values to previously published data of porcine and ovine ACU specimens with an axial preload of 0.4-0.5 Nm/° in flexion-extension, 0.5-1.1 Nm/° in lateral bending, and 0.9-1.2 Nm/° in axial rotation [6, 29], and lower than the pure moment testing of human ACU specimens without an axial preload of 1.5-1.8 Nm/° in flexion-extension, 2.0-2.1 Nm/° in lateral bending, and 2.0 Nm/° in axial rotation [28]. The effect of the flexion moment due to the axial preload is likely to be responsible for the deviations in the stiffness in flexion and extension compared to previous data, emphasizing that future studies should adjust the anteroposterior position to minimize

such artefacts. However, the general similarity in stiffness data provides confirmation that the results of the simulator are in line with the literature, despite the present study being limited to a single specimen. The tests were completed over normal ROMs, rather than physiological limits, though it will be possible in future studies to complete such tests.

Previous in-vivo studies have shown that posture alters the intradiscal pressure and increases the axial load through the spinal column [15, 21-23]. The intradiscal pressure at the L4-L5 level in human subjects was found to increase by 86-319 % from relaxed standing to approximately 5° of flexion, and a linear relationship was found between spinal load and intervertebral rotation [23]. Whilst there are limitations in comparing the result of the present study of a single ACU specimen against a FSU in-vivo, there are qualitative similarities of the present study with previous data. The axial load in the present study was found to increase by approximately 40% at 4° of flexion, and decrease by approximately 20 % at 4° of extension. The reduction in axial load in extension is related to the flexion moment created as a result of the preload application (Figure 3); a greater degree of extension, leading to an extension moment, would be likely to cause the axial load to increase. The adjustment of the anteroposterior position upon preload application described above, may lead to increases in axial load with extension in ACU specimens. However, previous studies report mixed results in terms of the effects of extension, with Sato et al [23] reporting that when in approximately 3° extension the intradiscal pressure, compared to relaxed standing, was reduced in three subjects, remained approximately the same for one subject, and increased in four subjects. This variation may be the result of differences in individual spinal geometry and kinematics, but may also relate to methodological differences such as the position of the pressure sensor within the disc. Wilke et al reported that the intradiscal pressure approximately doubled in flexion, but little change occurred in extension [21]. The changes in axial load during lateral bending and axial rotation are also qualitatively comparable to the previous data of Wilke et al [21], though the relative increase of just over 10 % in axial load was much smaller than the maximum increase in intradiscal pressure of approximately 50 % measured

by Wilke et al. The relatively small increases in axial load observed in the present study may be the result of the small ROM used compared to the large rotations of the entire spinal column used in-vivo, but it is also likely that the interaction of the facets may lead to the larger changes observed in-vivo, as the facets may guide the rotational motion so that the axial load is increased to a greater extent than in the present study.

The changes in axial load reported in the present study are important in terms of how in-vitro tests should best replicate the in-vivo environment. Many previous studies have not applied a physiological preload [28, 30-32], and those studies that do so whilst operating a test system to apply unconstrained moments generally adopt a constant axial load [16] or constant follower-load [4, 17-19]. Whilst the method of maintaining constant axial position has limitations in terms of the axial load diminishing over the applied cycles and more constraint in terms of the COR, it does appear to produce a variation in axial load over rotation cycles that is qualitatively similar to in-vivo data. It is possible that the use of this method, combined with a fluid bath at 37°C to mimic the in-vivo environment may minimize the reduction in axial load as test cycles accumulate, but the constraint of the COR in the axial direction would still need consideration. It has been shown that neither pure moments without a preload, nor a follower-load, accurately replicate in-vivo cervical spine motion, but that a combination of a follower-load and axial load does simulate in-vivo segmental motion in flexion-extension [33]. Recent studies using an ideal follower-load combined with an axial load have shown that complex loading can be applied to spinal specimens [13]. Therefore, it may be appropriate to investigate how such control systems may be used to better replicate the in-vivo environment, whether through the application of load commands, or position control of vertebral translation and rotation from in-vivo 3D imaging data [34]. However, it remains a challenge to obtain such input data in a generalized form, due to the variability between specimens during in-vitro tests and between human subjects during in-vivo studies.

CONCLUSIONS

The spine simulator used in the present study is capable of applying dynamic physiological loading conditions, and further research will investigate the use of dynamic load vectors to better represent the in-vivo environment, which has thus far been limited to at 0.35°/s in the sagittal plane [12, 13]. The results of the present study are promising in terms of such a development. This will aid the characterisation of both the natural spine, and spinal instrumentation, with the ultimate aim of improving the treatment of spinal injury and degeneration.

ACKNOWLEDGEMENTS

The authors would like to thank the Higher Education Investment Fund, The Enid Linder Foundation, and the University of Bath Alumni Fund for their support with this study.

CONFLICT OF INTEREST STATEMENT

The authors do not have any personal or financial relationships that could inappropriately influence this work. The Higher Education Investment Fund, The Enid Linder Foundation, and the University of Bath Alumni Fund provided financial support for the development of the spine simulator but were not involved in the design, implementation, analysis, or reporting of this study.

REFERENCES

- [1] Holsgrove TP, Nayak NR, Welch WC, Winkelstein BA. Advanced Multi-Axis Spine Testing: Clinical Relevance and Research Recommendations. *International Journal of Spine Surgery*. 2015;9:34.
- [2] Wilke HJ, Wenger K, Claes L. Testing criteria for spinal implants: recommendations for the standardization of in vitro stability testing of spinal implants. *European Spine Journal*. 1998;7:148-54.
- [3] Goel VK, Panjabi MM, Patwardhan AG, Dooris AP, Serhan H. Test protocols for evaluation of spinal implants. *Journal of Bone and Joint Surgery-American Volume*. 2006;88 Suppl 2:103-9.
- [4] Patwardhan AG, Havey RM, Meade KP, Lee B, Dunlap B. A follower load increases the load-carrying capacity of the lumbar spine in compression. *Spine*. 1999;24:1003-9.
- [5] Gardner-Morse MG, Stokes IA. Physiological axial compressive preloads increase motion segment stiffness, linearity and hysteresis in all six degrees of freedom for small displacements about the neutral posture. *Journal of Orthopaedic Research*. 2003;21:547-52.
- [6] Holsgrove TP, Gill HS, Miles AW, Gheduzzi S. The dynamic, six-axis stiffness matrix testing of porcine spinal specimens. *The Spine Journal*. 2015;15:176-1884.
- [7] Costi JJ, Stokes IA, Gardner-Morse MG, Iatridis JC. Frequency-dependent behavior of the intervertebral disc in response to each of six degree of freedom dynamic loading - Solid phase and fluid phase contributions. *Spine*. 2008;33:1731-8.
- [8] Gay RE, Ilharreborde B, Zhao K, Boumediene E, An KN. The effect of loading rate and degeneration on neutral region motion in human cadaveric lumbar motion segments. *Clinical Biomechanics*. 2008;23:1-7.
- [9] Wilke HJ, Claes L, Schmitt H, Wolf S. A universal spine tester for in vitro experiments with muscle force simulation. *European Spine Journal*. 1994;3:91-7.
- [10] Wilke HJ, Kienle A, Maile S, Rasche V, Berger-Roscher N. A new dynamic six degrees of freedom disc-loading simulator allows to provoke disc damage and herniation. *European Spine Journal*. 2016;25:1363-72.

364 [11] Oxland TR. Fundamental biomechanics of the spine-What we have learned in the past
 365 25 years and future directions. *Journal of Biomechanics*. 2015.

366 [12] Bennett CR, Kelly BP. Robotic application of a dynamic resultant force vector using real-
 367 time load-control: Simulation of an ideal follower load on Cadaveric L4–L5 segments.
 368 *Journal of Biomechanics*. 2013;46:2087-92.

369 [13] Bennett CR, DiAngelo DJ, Kelly BP. Biomechanical comparison of robotically applied
 370 pure moment, ideal follower load, and novel trunk weight loading protocols on L4-L5
 371 cadaveric segments during flexion-extension. *International Journal of Spine Surgery*.
 372 2015;9:33.

373 [14] Nachemson AL. Disc pressure measurements. *Spine*. 1981;6:93-7.

374 [15] Wilke HJ, Neef P, Caimi M, Hoogland T, Claes LE. New in vivo measurements of
 375 pressures in the intervertebral disc in daily life. *Spine*. 1999;24:755-62.

376 [16] Mahomed A, Moghadas PM, Shepherd DE, Hukins DW, Roome A, Johnson S. Effect of
 377 axial load on the flexural properties of an elastomeric total disc replacement. *Spine*.
 378 2012;37:E908-12.

379 [17] Zirbel SA, Stolworthy DK, Howell LL, Bowden AE. Intervertebral disc degeneration
 380 alters lumbar spine segmental stiffness in all modes of loading under a compressive follower
 381 load. *The Spine Journal*. 2013;13:1134-47.

382 [18] Fry RW, Alamin TF, Voronov LI, Fielding LC, Ghanayem AJ, Parikh A, et al.
 383 Compressive preload reduces segmental flexion instability after progressive destabilization
 384 of the lumbar spine. *Spine*. 2014;39:E74-81.

385 [19] Yan Y, Bell KM, Hartman RA, Hu J, Wang W, Kang JD, et al. In vitro evaluation of
 386 translating and rotating plates using a robot testing system under follower load. *European*
 387 *Spine Journal*. 2015, in press. DOI: 10.1007/s00586-015-4203-8.

388 [20] Lawless IM, Ding B, Cazzolato BS, Costi JJ. Adaptive velocity-based six degree of
 389 freedom load control for real-time unconstrained biomechanical testing. *Journal of*
 390 *Biomechanics*. 2014;47:3241-7.

391 [21] Wilke H, Neef P, Hinz B, Seidel H, Claes L. Intradiscal pressure together with
392 anthropometric data--a data set for the validation of models. *Clinical Biomechanics*. 2001;16
393 Suppl 1:S111-26.

394 [22] Nachemson A, Morris JM. In Vivo Measurements of Intradiscal Pressure. *Discometry, a*
395 *Method for the Determination of Pressure in the Lower Lumbar Discs*. *Journal of Bone and*
396 *Joint Surgery-American Volume*. 1964;46:1077-92.

397 [23] Sato K, Kikuchi S, Yonezawa T. In vivo intradiscal pressure measurement in healthy
398 individuals and in patients with ongoing back problems. *Spine*. 1999;24:2468-74.

399 [24] Holsgrove TP, Gheduzzi S, Gill HS, Miles AW. The development of a dynamic, six-axis
400 spine simulator. *The Spine Journal*. 2014;14:1308-17.

401 [25] Dvorak J, Panjabi MM, Chang DG, Theiler R, Grob D. Functional radiographic diagnosis
402 of the lumbar spine. Flexion-extension and lateral bending. *Spine*. 1991;16:562-71.

403 [26] White AA, 3rd, Panjabi MM. The basic kinematics of the human spine. A review of past
404 and current knowledge. *Spine*. 1978;3:12-20.

405 [27] Stokes IA, Gardner-Morse M, Churchill D, Laible JP. Measurement of a spinal motion
406 segment stiffness matrix. *Journal of Biomechanics*. 2002;35:517-21.

407 [28] Spenciner D, Greene D, Paiva J, Palumbo M, Crisco J. The multidirectional bending
408 properties of the human lumbar intervertebral disc. *The Spine Journal*. 2005;6:248-57.

409 [29] Costi JJ, Hearn TC, Fazzalari NL. The effect of hydration on the stiffness of
410 intervertebral discs in an ovine model. *Clinical Biomechanics*. 2002;17:446-55.

411 [30] Martínez H, Obst T, Ulbrich H, Burgkart R. A novel application of direct force control to
412 perform in-vitro biomechanical tests using robotic technology. *Journal of Biomechanics*.
413 2013;46:1379-82.

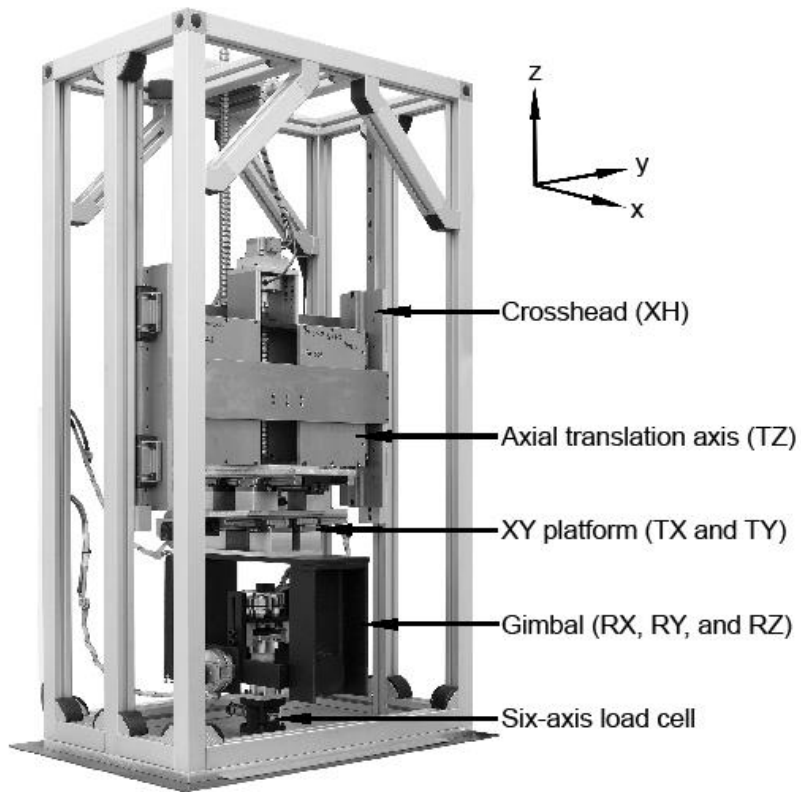
414 [31] Bell KM, Hartman RA, Gilbertson LG, Kang JD. In vitro spine testing using a robot-
415 based testing system: Comparison of displacement control and "hybrid control". *Journal of*
416 *Biomechanics*. 2013;46:1663-9.

417 [32] Kelly BP, Bennett CR. Design and validation of a novel Cartesian biomechanical testing
418 system with coordinated 6DOF real-time load control: application to the lumbar spine (L1–S,
419 L4–L5). *Journal of Biomechanics*. 2013;46:1948-54.

420 [33] Bell KM, Yan Y, Debski RE, Sowa GA, Kang JD, Tashman S. Influence of varying
421 compressive loading methods on physiologic motion patterns in the cervical spine. *Journal*
422 *of Biomechanics*. 2015;49:167-72.

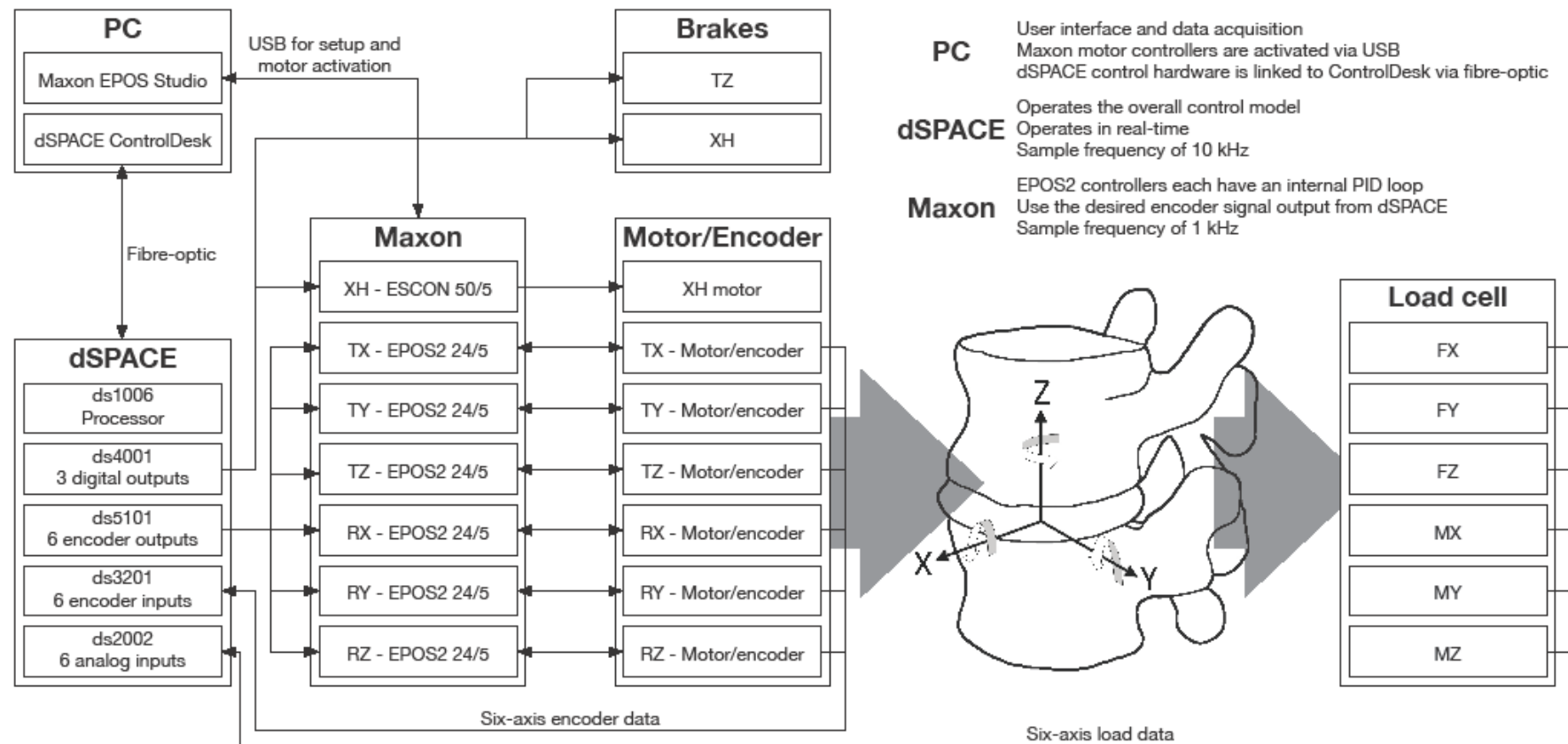
423 [34] Goel VK, Wilder DG, Pope MH, Edwards WT. Biomechanical testing of the spine. Load-
424 controlled versus displacement-controlled analysis. *Spine*. 1995;20:2354-7.

425



427

428 Figure 1. The six-axis spine simulator



429

430 Figure 2. Schematic of the control architecture of the spine simulator

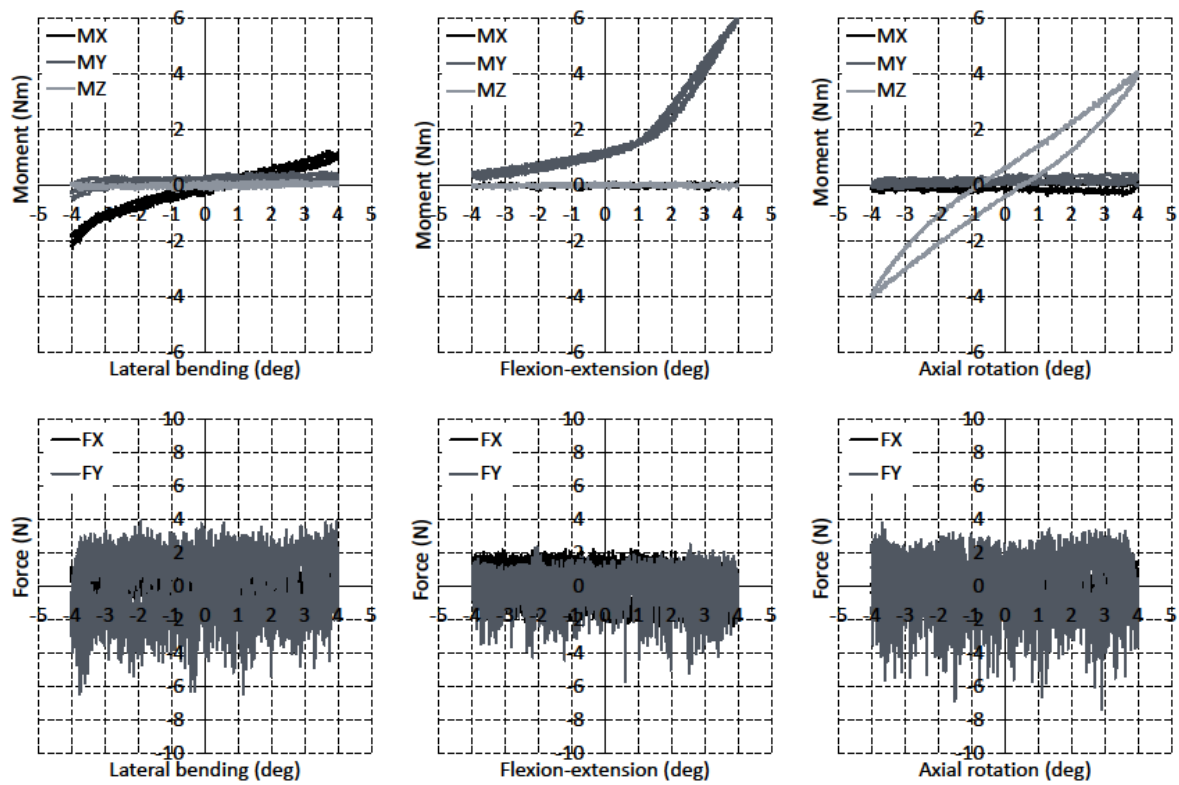
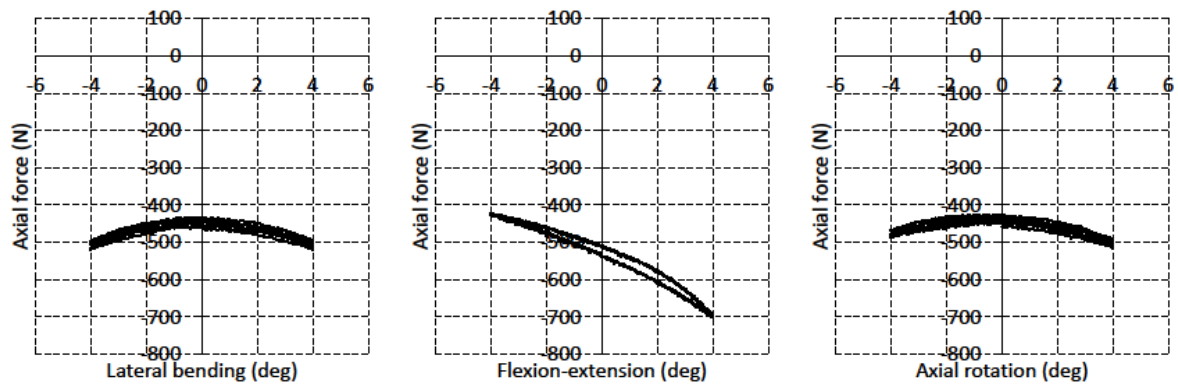


Figure 3: Variation of moments (top row) and shear forces (bottom row) in lateral bending (left), flexion-extension (centre), and axial rotation (right) over the last three test cycles at 0.1 Hz. Moments shown are in the direction of lateral bending (MX), flexion-extension (MY), and axial rotation (MZ). Shear forces shown are in the direction of anterior-posterior (FX), and lateral (FY).



437

438

Figure 4: Variation of axial load as a result of rotation in lateral bending (left), flexion-

439

extension (centre), and axial rotation (right) over the last three test cycles at 0.3 Hz

440 **LIST OF TABLES**

441 Table 1. Summary of recent in-vitro spine testing systems with active six-axis control

Study	Preload	Test rate	Primary axis	Primary axis control	Zero load RMS error	Zero moments RMS error
[30]	0 N	~0.86 Hz (0.086-0.131 °/s)	Flexion-extension	Load	1.18 N	0.14 Nm
			Lateral bending	Load	0.85 N	0.14 Nm
			Axial rotation	Load	0.72 N	0.14 Nm
[32]	0 N	0.1-0.35 Nm/s (0.15-0.5 °/s)	Flexion-extension	Load	0.61 N	0.02 Nm
			Lateral bending	Load	0.56 N	0.02 Nm
			Axial rotation	Load	0.56 N	0.02 Nm
[31]	10 N AL	0.067 °/s	Flexion-extension	Hybrid	1.71 N	0.11 Nm
			Lateral bending	Hybrid	1.71 N	0.11 Nm
			Axial rotation	Hybrid	1.71 N	0.11 Nm
[12]	400 N IFL	0.35 °/s	Flexion-extension	Position	0.70 N	0.03 Nm
[20]	0.2 MPa IFL	0.01 Hz	Flexion-extension	Load	9.78 N	0.11 Nm
		0.01 Hz	Lateral bending	Load	6.82 N	0.23 Nm
		0.30 Hz	Axial rotation	Load	11.7 N	0.43 Nm
[13]	400 N AL	0.35 °/s	Flexion-extension	Position	~3 N	~0.05 Nm
	400 N IFL	0.35 °/s	Flexion-extension	Position		

442 Notes on the preload application methods: Axial load (AL), and ideal follower-load (IFL)

443 Table 2: Electromechanical drive assemblies for each axis of the spine simulator, and the crosshead (XH)

Axis	Drive Assembly	Parts	Accuracy	Resolution	Speed	ROM	Load
TX	<ul style="list-style-type: none"> - Two parallel linear guide rails - Ball screw assembly - Coupling - Brushless motor - Digital Encoder 	<ul style="list-style-type: none"> - HSR25B2SS, THK UK, Milton Keynes, UK - BNK1202, THK UK - GESM, Lenze Ltd., Bedford, UK - EC90, Maxon Motor UK Ltd., Finchampstead, UK - HEDL 5540, Maxon Motor UK 	± 0.018 mm	± 0.001 mm	± 20 mm/s	± 90 mm	± 500 N
TY	<ul style="list-style-type: none"> - Two parallel linear guide rails - Ball screw assembly - Coupling - Brushless motor - Digital Encoder 	<ul style="list-style-type: none"> - HSR25B2SS, THK UK, - BNK1202, THK UK - GESM, Lenze - EC90, Maxon Motor UK - HEDL 5540, Maxon Motor UK 	± 0.018 mm	± 0.001 mm	± 20 mm/s	± 90 mm	± 500 N
TZ	<ul style="list-style-type: none"> - Two parallel linear guide rails - Ball screw assembly - Coupling - Harmonic Drive servo-actuator and digital encoder - Brake 	<ul style="list-style-type: none"> - HSR35BCSS, THK UK - EBB2505, THK UK - GS14, KTR Kupplungstechnik GmbH, Rheine, Germany - FHA-11C-50-D200-EM1, Harmonic Drive UK Ltd., Stafford, UK - BFK457-06, Intorq GmbH & Co KG, Aerzen, Germany 	± 0.023 mm	± 0.0125 μ m	± 10 mm/s	± 90 mm	± 4000 N
RX	<ul style="list-style-type: none"> - Harmonic Drive Gear assembly with brushless motor and digital encoder - Non-drive-side support bearing 	<ul style="list-style-type: none"> - HFUC-17-80-2UH-SP+EC90+HEDL5540, Harmonic Drive UK - 6200 ZRSH, AB SKF, Gothenburg, Sweden 	$\pm 0.0025^\circ$	$\pm 0.00225^\circ$	$\pm 45^\circ/\text{s}$	$\pm 45^\circ$	± 35 Nm
RY	<ul style="list-style-type: none"> - Harmonic Drive Gear assembly with brushless motor and digital encoder - Non-drive-side support bearing 	<ul style="list-style-type: none"> - HFUC-17-80-2UH-SP+EC90+HEDL5540, Harmonic Drive UK - 6200 ZRSH, AB SKF 	$\pm 0.0025^\circ$	$\pm 0.00225^\circ$	$\pm 45^\circ/\text{s}$	$\pm 45^\circ$	± 35 Nm
RZ	<ul style="list-style-type: none"> - Harmonic Drive Gear assembly with brushless motor and digital encoder 	<ul style="list-style-type: none"> - HFUC-17-80-2UH-SP+EC90+HEDL5540, Harmonic Drive UK 	$\pm 0.0025^\circ$	$\pm 0.00225^\circ$	$\pm 45^\circ/\text{s}$	$\pm 45^\circ$	± 35 Nm
XH	<ul style="list-style-type: none"> - Two parallel linear guide rails - Ball screw assembly - Coupling - Brushless motor - Planetary gearhead - Brake 	<ul style="list-style-type: none"> - HSR35BCSS, THK UK - EBB2505, THK UK - GS14, KTR Kupplungstechnik GmbH - EC45, Maxon Motor UK - GP32A, 166167, Maxon Motor UK - BFK457-06, Intorq GmbH & Co KG 			± 1 mm/s	± 90 mm	

444 Table 3: Mean (standard deviation) RMS tracking error for primary axes, and RMS load error for zero load demand on non-primary axes for
 445 each of the last three cycles applied to a porcine lumbar ACU specimen. Italics denote cases in which the RMS load error was not maintained
 446 within two-times the load cell noise-floor of 5 N and 0.25 Nm

----- Test parameters -----			----- RMS error -----					
Primary Axis	Freq (Hz)	Preload (N)	Tracking (deg)	FX (N)	FY (N)	MX (Nm)	MY (Nm)	MZ (Nm)
RX	0.1	500	0.005(0.000)	0.307(0.012)	1.600(0.026)		0.189(0.097)	0.060(0.003)
RY	0.1	500	0.005(0.000)	1.158(0.001)	0.775(0.054)	0.035(0.001)		0.034(0.001)
RZ	0.1	500	0.007(0.000)	0.331(0.015)	1.376(0.025)	0.141(0.001)	0.165(0.102)	
RX	0.3	500	0.010(0.001)	0.390(0.021)	4.050(0.021)		<i>0.630(0.097)</i>	0.150(0.002)
RY	0.3	500	0.014(0.001)	3.144(0.077)	0.912(0.077)	0.050(0.006)		0.040(0.005)
RZ	0.3	500	0.011(0.001)	0.433(0.043)	3.218(0.038)	0.362(0.005)	<i>0.560(0.090)</i>	

447 Table 4: Mean (SD) stiffness of the porcine ACU specimen for each of the last three cycles

Test axis	Stiffness (Nm/°)		R ²	
	0.1 Hz	0.3 Hz	0.1 Hz	0.3 Hz
Flexion	1.28(0.02)	1.47(0.02)	0.945(0.005)	0.967(0.003)
Extension	0.20(0.00)	0.15(0.00)	0.829(0.004)	0.243(0.005)
Lateral Bending	0.35(0.07)	0.31(0.03)	0.893(0.016)	0.483(0.063)
Axial Rotation	0.97(0.02)	1.07(0.02)	0.858(0.002)	0.869(0.007)

448

449 Table 5: Mean (SD) stiffness relating to the axial load and rotations about each axis on the
 450 porcine ACU specimen for each of the last three cycles

Test axis	Stiffness (N/°)		R ²	
	0.1 Hz	0.3 Hz	0.1 Hz	0.3 Hz
Flexion	-41.18(0.37)	-42.91(0.58)	0.921(0.001)	0.927(0.002)
Extension	24.86(0.28)	24.44(0.35)	0.920(0.001)	0.928(0.007)
Lateral Bending	-13.19(0.55)	-14.98(0.59)	0.871(0.037)	0.894(0.023)
Axial Rotation	-12.87(2.32)	-12.32(2.92)	0.820(0.028)	0.852(0.034)

451